

**Prediction of Weld Metal Strength**  
**(Report III)**

**N. Yurioka**

**Nippon Steel Corporation, Technical Development Bureau**  
**20-1, Shintomi, Futtsu-City, Chiba-Pref. 293-8511 JAPAN**

**Abstract**

The Sub-Commission IX-J made a database of weld metal properties and chemical compositions. The database includes 101 sets of SAW, 174 sets of GMAW, and 49 sets of SMAW. Based on this database and a weld metal database from a website of University of Cambridge, a formula predicting weld metal tensile strengths was proposed. This formula was verified to estimate the tensile strength of SAW, GMAW, and SMAW weld metals from a mild steel grade to 980MPa grade under welding conditions of arc energy from 1.0 to 14kJ/mm and inter-pass temperature from 20 to 450°C with satisfactory accuracy.

## 1. Introduction

A weld metal database is being built in the IIW Sub-Commission IX-J (Metallurgical Behavior of Fused Metal). This database includes 49 sets of SMAW, 174 sets of GMAW and 101 sets of SAW<sup>1)</sup>. There is another database that is available in a website provided by Prof. B. H. D. Bhadeshia, University of Cambridge<sup>2)</sup>. There are 1,254 sets of SMAW, 281 sets of SAW and 85 sets of FCAW weld metals in the U. Cambridge database, Both database provide us welding condition, chemical composition, hardness, yield strength, tensile strength, elongation, and FATT. The U. Cambridge database provides a volume fraction of phases of martensite, upper-bainite, primary ferrite, secondary ferrite, and acicular ferrite for a part of weld metals.

It is not easy task to predict weld metal properties. Recently, this predictive work is vigorously carried out by means of a neural network analysis<sup>3,4)</sup>. A Bayesian neural network analysis among analyses enables to provide an estimation error range<sup>3,4)</sup>. However, the neural network analysis does not indicate a physical meaning of their prediction, such as effects of alloy elements on hardenability or precipitation hardening.

Four years work in the IIW SCIX-J has suggested that a predictive formula for the hardness and tensile strength of weld metals can be built but not for the yield strength and toughness. This report describes a predictive equation formulated based upon both the IIW SCIX-J database and the U. Cambridge database.

## 2. Database

Tables 1 to 5 show the databases used in this study. Although the mother databases include Charpy properties, the Tables show only tensile test results. Table 1 shows an IIW SCIX-J database of SAW weld metals<sup>5)</sup>. Table 2 is a U. Cambridge database of SAW weld metals of as-welded and dehydrogen-heat-treated at around 200°C, while the data of weld metals subjected to PWHT being excluded.

Table 3 is a database of solid wire GMAW weld metals. The data denoted by NSW come from the catalogue data by Nippon Steel Welding Materials

Co<sup>6)</sup>, and the data from No.22 to No.29 are from Nippon Steel Labs<sup>7)</sup>. The others are from a report of the investigation of the effects of the arc energy and inter-pass temperature on mechanical properties of weld metals for building construction<sup>8)</sup>. Among these, the data from No.31 to 86 are for JIS (Japan Industrial Standard) Z YGW12 of a TS490MPa grade, those from No.87 to No.126 are for JIS Z YGW17 of a TS540MPa, and those from No.127 to No.174 are for JIS Z YGW21 of a TS580MPa grade.

Table 4 is a database of SMAW weld metals, including those from a NSW catalogue<sup>6)</sup> and those from Kobelco report<sup>9)</sup>. Catalogues of welding materials do not, in general, show arc energy values but those shown in Table 4 are by private communication<sup>10)</sup>. Table 5 is a U. Cambridge database of SMAW as welded and as dehydrogen heat-treated. The data from No.1085 to No.1100 in Table 5 is given as as-welded but the original paper<sup>11)</sup> of the U. Cambridge database described the tensile tests results were from weld metals dehydrogen heat-treated at 250°C for 14hrs while Charpy test results being from those as-welded. Therefore, these data are considered for weld metals dehydrogen heat-treated in Table 5.

The welding cooling times from 800°C to 500°C,  $t_{8/5}$ (s) were calculated in a equation shown in Appendix, where the arc efficiency,  $\eta$  is 1.0 for SAW and 0.8 for SMAW and GMAW.

### 3. Predictive formula

It is known that a preferable correlation between the tensile strength and hardness holds. The following is one example<sup>5)</sup>:

$$TS(\text{MPa}) = 3.0 \text{ Hv} + 22.3 \quad (1)$$

In this study, a following predictive formula for base metal HAZ hardness<sup>12)</sup> was employed for predicting weld metal hardness:

$$H_V = \frac{H_M + H_B}{2} - \frac{H_M - H_B}{2.2} \arctan(x) \quad (2)$$

$$x = 4 \frac{\log(t_{8/5}/t_M)}{\log(t_B/t_M)} - 2 \quad (3)$$

where,  $H_M$ : hardness of 100% martensite phase,

$H_B$ : hardness of 0% martensite phase,

$t_{8/5}$ : welding cooling times from 800°C to 500°C (s),

$t_M$ : longest cooling time to get 100% martensite phase (s),

$t_B$ : shortest cooling time to get 0% martensite phase (s).

The martensite hardness is determined solely by the carbon content and the following relation holds<sup>12)</sup> in HAZ. It is assumed that the same relation holds in weld metals.

$$H_M = 884C + 294 \quad (4)$$

$t_M$  is considered as an index for hardenability. In this study,  $t_M$  was given by Eq. (5) as a function of carbon equivalency of Eq. (6) which was obtained by a best fitting manner against the present database:

$$t_M = \exp(10.6CE_I - 4.8) \quad (5)$$

$$CE_I = C + \frac{Si}{24} + \frac{Mn}{288(1+Mn)} + \frac{Ni}{30} + \frac{Cr}{16} + \frac{Mo}{8} \quad (6)$$

In Eq.(6), the effect of Mn is non-linear as indicated as Mn/(1+Mn). This means that activity of Mn decreases as a Mn content increases. Ni and Cr are considered to show the same tendency, but their effects were considered in this study to be linear for Ni less than 3.5% and Cr less than 1.25% as indicated by the present database. Cu was considered to not contribute to hardenability but only to precipitation hardening. Thus, Cu was ignored in Eq.(6). The hardenability effects of Mn, Cu, Ni, Cr, and Mo will be discussed later.

$H_B$  is the hardness of 0% martensite phase plus that due to precipitation hardening which arises only when  $t_{8/5}$  becomes long. That was given by Eq.(7) as a function of a carbon equivalency of Eq.(8) in which the effect of precipitation hardening elements of Cu, Mo, V, Nb, Ti are relatively high. The non-linear effect of Nb was considered as 2.2Nb/(1+5Nb) in Eq.(8). These effect will be discussed later.

$$H_B = 145 + 130 \tanh(2.65CE_{II} - 0.69) \quad (7)$$

$$CE_{II} = C + \frac{Si}{24} + \frac{Mn}{216(1+Mn)} + \frac{Cu}{10} + \frac{Ni}{45} + \frac{Cr}{10} + \frac{Mo}{5} + 2V + \frac{2.2Nb}{(1+5Nb)} + \frac{Ti}{10} \quad (8)$$

$t_B$  is the critical cooling time when martensite phases diminish and considered as an index of easiness of bainite formation. That was given by Eq.(9) as a function of carbon equivalency of Eq.(1):

$$t_B = \exp(6.2CE_{III} + 0.74) \quad (9)$$

$$CE_{III} = C + \frac{Mn}{168(1+Mn)} + \frac{Ni}{15} + \frac{Cr}{10} + \frac{Mo}{8} \quad (10)$$

As described above, the weld metal tensile strength can be predicted through Eq.(1) from the hardness estimated through Eq. (2) as a function

of  $t_{8/5}$  (Appendix) and chemical compositions via Eqs. (3) to (10). The applicable range in the alloy element concentration is  $C < 0.10\%$  •  $Si < 1.15\%$  •  $Mn < 2.0\%$  •  $Cu < 1.5\%$  •  $Ni < 3.5\%$  •  $Cr < 2.25\%$  •  $Mo < 1.2\%$  •  $Nb < 0.10\%$  •  $V < 0.10\%$ , and that in the welding condition is  $5s < t_{8/5} < 160s$ .

#### 4. Accuracy of prediction

$t_{8/5}$  must be estimated from the welding conditions (Appendix) before predicting the tensile strength. Accuracy of this prediction totally depends on that of  $t_{8/5}$  estimation and the precision of  $t_{8/5}$  estimation is described in Appendix. The plate thickness is not mentioned in the U. Cambridge database and 20mm thickness was considered for the whole data of U. Cambridge.

Figs. 1 to 5 show hardness estimated by the present predictive formula and that from the present database. The prediction in this study is considered satisfactory except for the data of higher strength weld metals of SAW of U. Cambridge database shown in Fig.2 and those of de-hydrogen heat-treated SMAW of U. Cambridge database shown in Fig.5. The SMAW weld metals shown in Fig. 5 were heat-treated at 200°C or 250°C for 10hrs or more for removing hydrogen from tensile test pieces. The duration of heat treatment seems too long for de-hydrogen. It is thus presumed that the measured values are considerably less than those predicted as shown in Fig.5.

In the database of solid wire GMAW for building constructions, welding conditions were varied considerably between 1.0kJ/mm and 4.0kJ/mm in arc energy (AE) and up to 450°C in inter-pass temperature (IP)<sup>8)</sup>. The resultant  $t_{8/5}$  was between 10s and 160s. Figs. 6, 7 and 8 shows the results of the prediction for GMAW weld metals, where solid lines were given only for the measured data. Accuracy of the prediction was between -10MPa and +50MPa, i.e., somewhat higher values were predicted under the wide range of welding conditions.

#### 5. Discussion

The U. Cambridge database of SMAW include the effect of concentration of Mn, Cu, Ni, Cr, Mo, Nb and V on mechanical properties while keeping the welding condition and the concentration of other elements unchanged, although these data are available only for the weld metals de-hydrogen

treated with rather longer duration. Using these data this study investigated the validity of the significance of each element on hardenability and precipitation hardening, i.e., coefficients in carbon equivalent equations of Eqs.(6), (8), and (10).

Fig.9 shows the effect of Mn on both the predicted tensile strength and that (connected by solid lines or dotted lines) of the database. The database values increases in almost a linear manner while the predicted ones are lower in the low Mn region and higher in the high Mn region. This is because the Mn effect was considered as  $Mn/(1+Mn)$  in the carbon equivalents of Eqs. (6), (8), and (10). As far as the U. Cambridge SMAW database is concerned, the effect of Mn on weld metal strength seems to be linear.

However, accuracy of the prediction was considerably degraded for the SAW data, GMAW data, and SMAW data other than the U. Cambridge SMAW data if the Mn effect was considered linear. For example, the prediction and measurement was compared between when the Mn effect is linear and that is non-linear of  $Mn/(1+Mn)$  as shown in Fig.10. In the case of the linear effect, significantly lower values in the prediction resulted and in the non-linear case, preferable prediction resulted. In this study, therefore, the effect of Mn on weld metal tensile strength was considered non-linear.

Fig.10 shows the effect of Cu, which was considered in the present prediction to influence only precipitation hardening but not hardenability. Although higher values are predicted against weld metals with high Mn (long-time de-hydrogen treated), gradients of the tensile strength against the Cu contents preferably coincides between prediction and the database. It is reported that the Cu effect on the tensile strength emerges only when Cu is over 0.5%<sup>13)</sup>. In fact, little effects of Cu not higher than 0.5% are seen in Fig.10.

Fig.11 shows the effect of Ni. Higher values are also predicted against weld metals with high Mn. It seems that the predicted effect of Ni is strong against the U. Cambridge data to some extent. However, the prediction against the other database was improved with the coefficients given in Eqs. (6), (8) and (10).

Fig.12 shows the effect of Cr. Although the higher prediction resulted against high Mn weld metals long-time de-hydrogen treated, the

gradients of the tensile strengths predicted vs. the Cr content satisfactorily coincided with those of the database.

Fig.13 shows the effect of V. In the prediction, V was considered to contribute only to precipitation hardening like Cu. Although the higher prediction resulted again against high Mn weld metals, the gradient of the tensile strengths vs. the V content satisfactorily coincided with those of the database.

Fig.14 shows the effect of Nb, which was considered to contribute only to precipitation hardening like Cu and V. In the U. Cambridge data, the effect of Nb on the tensile strength decreases with increasing Nb content. Therefore, the Nb terms in Eq.(8) was considered as  $Nb/(1+5Nb)$ . As a result, the gradients of the tensile strengths predicted vs. the Nb content satisfactorily coincided with those of the database although the higher values were predicted against the high Mn weld metals.

## 6. Conclusion

The effect of alloying elements on hardness, hardenability, and precipitation hardening of weld metals was investigated using the IIW IX-J database and the U. Cambridge database. Through this investigation, a formula predicting the hardness and tensile strength of a weld metal was proposed. This formula was verified to satisfactorily predict the hardness and tensile strength of weld metals from a mild steel grade to a TS1,000MPa high strength grade under the welding condition from 1.0kJ/mm to 14.0kJ/mm in arc energy and up to 450°C in inter-pass temperature.

## References

- 1) N. Yurioka : Prediction of Strength of Weld Metal (Report II), IIW Doc. IX-2026-02  
(2002)
- 2) Materials Algorithms Project,  
<http://www.msm.cam.ac.uk/map/data/materials/welddb-b.html>
- 3) H. K. D. H. Bhadeshia, D. J. C. MacKay, L. E. Svensson : Impact Toughness of C-Mn Steel Arc Welds - Bayesian Neural Network Analysis, Material Science and Technology, 11 (1995), p.1046
- 4) T. Cool, H. K. D. H. Bhadeshia, D. J. C. MacKay : The Yield and Ultimate

Tensile Strength of Steel Welds, Materilas Science & Engineering, A, A223 (1997), p.186

5) N. Yurioka, M. Wakabayashi, R. Motomatsu : Data Sheet of Mechanical Properties of SAW Weld Metals, IIW Doc. IX-1868-97(1997)

6) NITTETSU Catalogue of welding materials and welding machines: Nippon Steel Welding Products Co.

7) S. Ohkita and K. Koyama: Private communication

8) Research Report on proper welding conditions and welding materials in building constructions, AW Accreditation Committee, March 2001 (in Japanese)

9) H. Hatano, M. Otsu, T.Sugino, N. Hara: Effect of Ti on Microstructurres of High Strength Weld, Preprints of National Meeting of JWS, No.68, (Spring, 2001), p.162, in Japanese

10) K. Yamane: Private communication

11) G. M. Evans : Effect of Interpass Temperature on the microstructure and Properties of C-Mn All-weld-metal Deposits, IIW Doc. II-A-460-78

12) N. Yurioka, M. Okumura. T. Kasuya, H. J. U. Cotton: Prediction of HAZ Hardness of Ferritic Steels, Metal Constr., (1987), p.217R-273R

13) Dearden and H. O'Neill : A Guide to the Selection and Welding of Low Alloy Structural Steels, Institute of Welding Transactions, 3 (1940), p.203



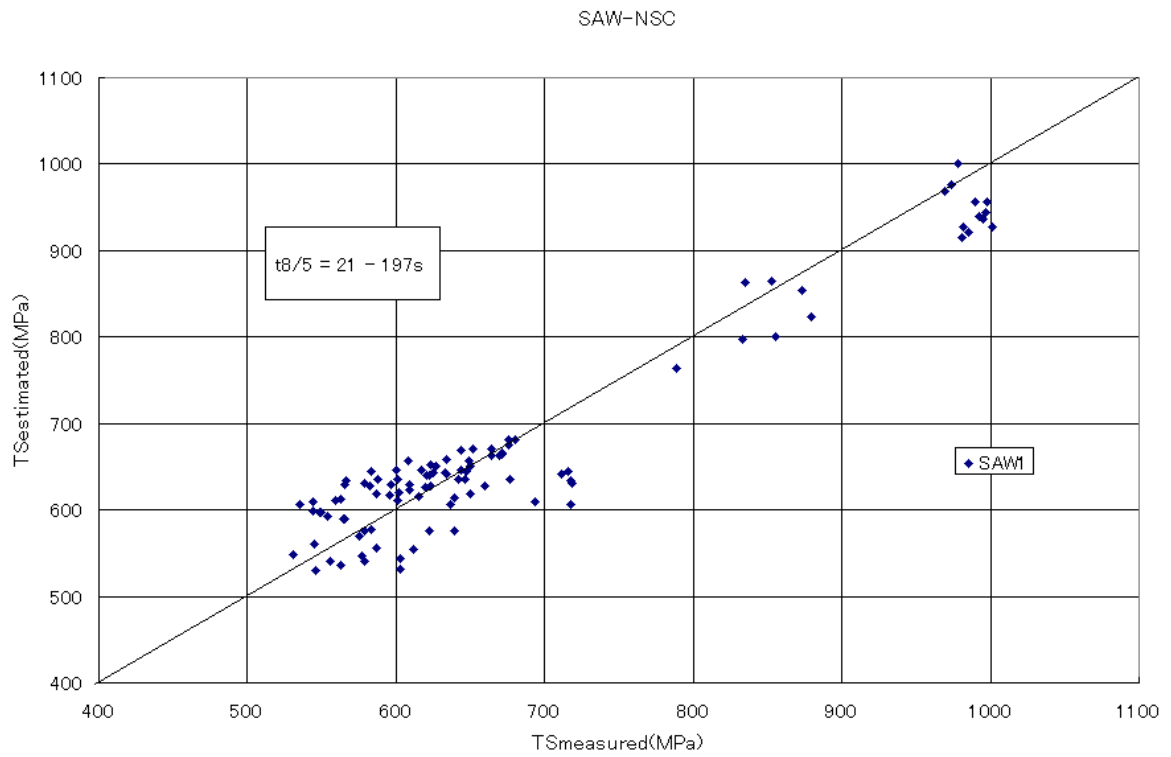


Fig. 1 SAW weld metal tensile strengths measured and predicted

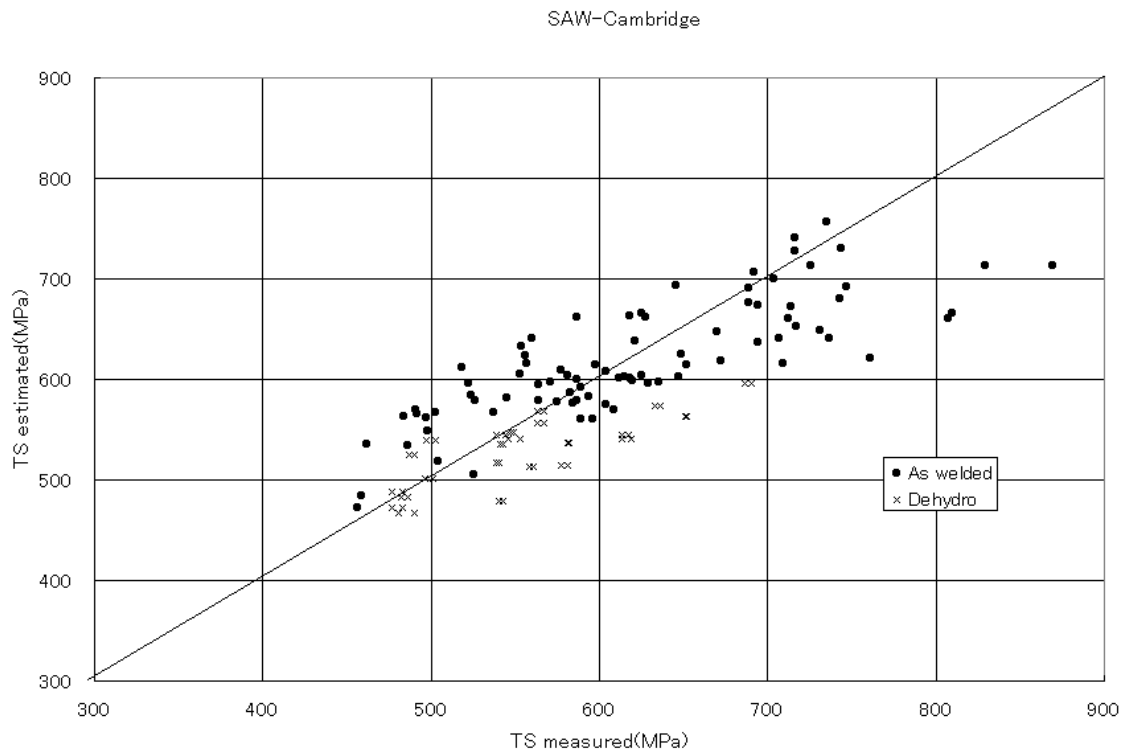


Fig.2 SAW (U. Cambridge) weld metal tensile strengths) measured and predicted

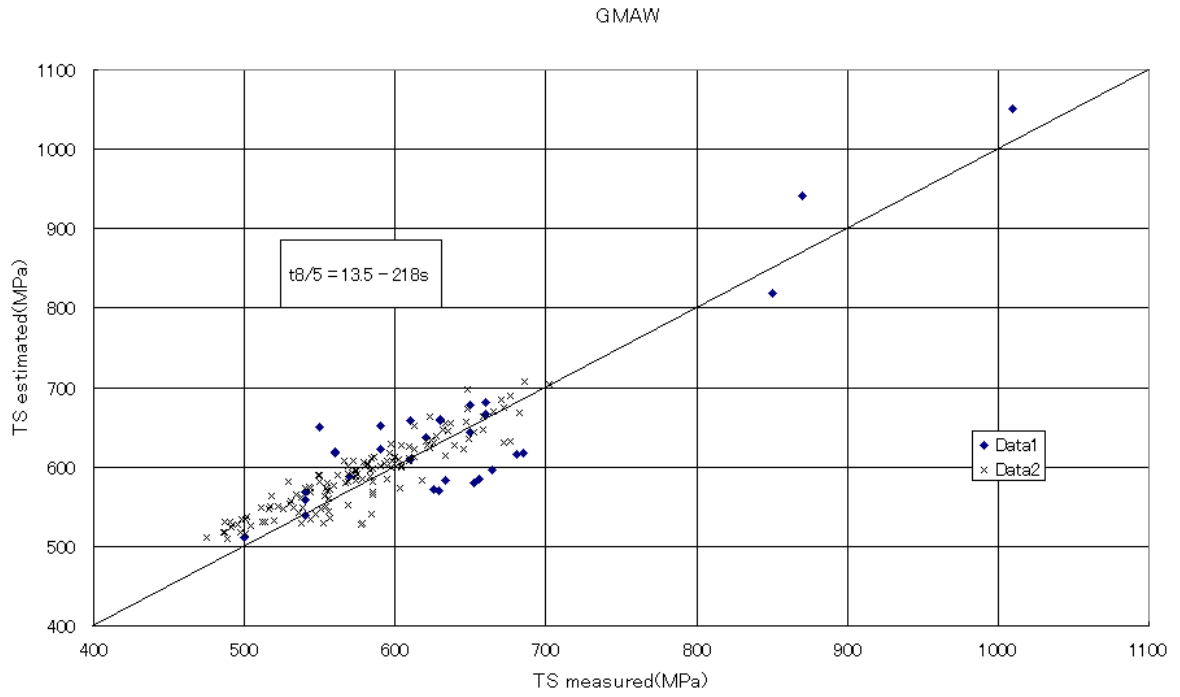


Fig.3 GMAW weld metal tensile strengths measured and predicted

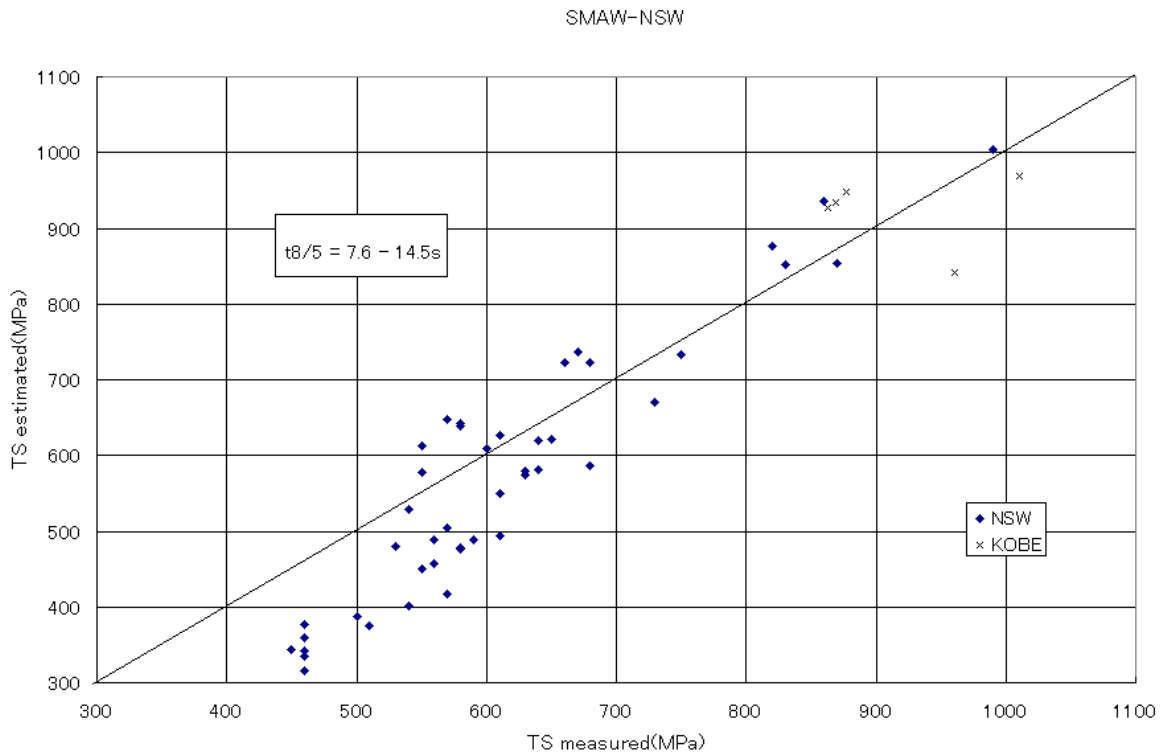


Fig.4 SMAW weld metal tensile strengths measured and predicted

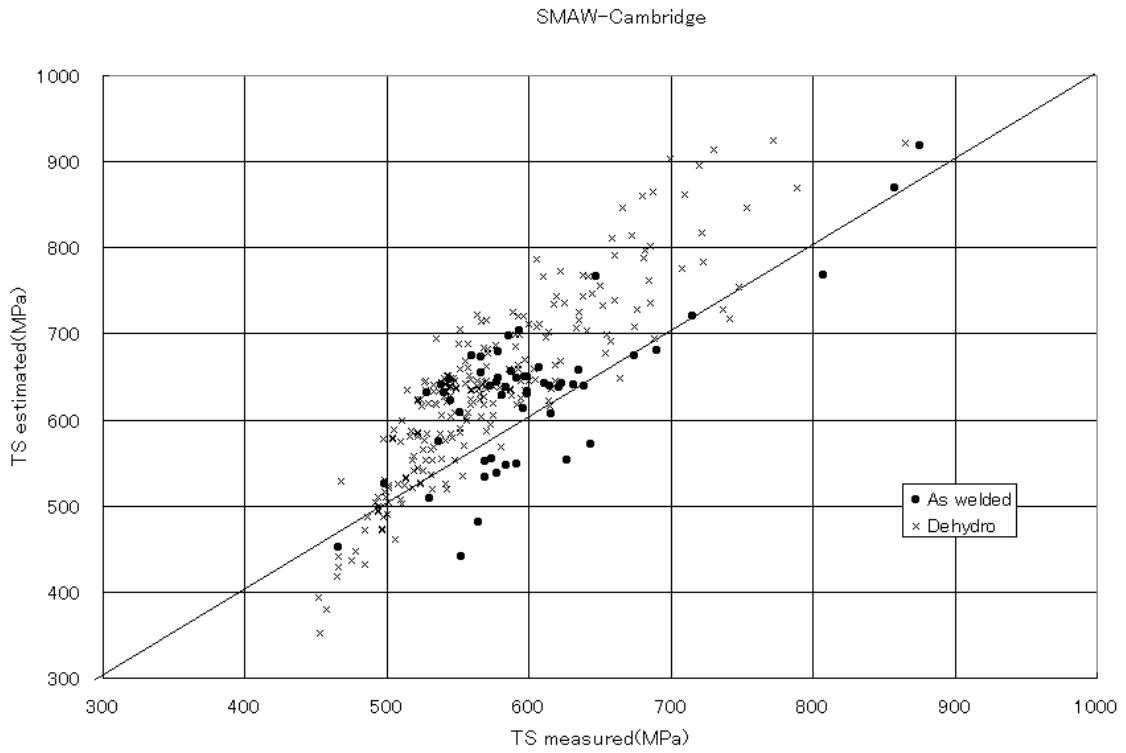


Fig.5 SMAW (U. Cambridge) weld metal tensile strengths measured and predicted

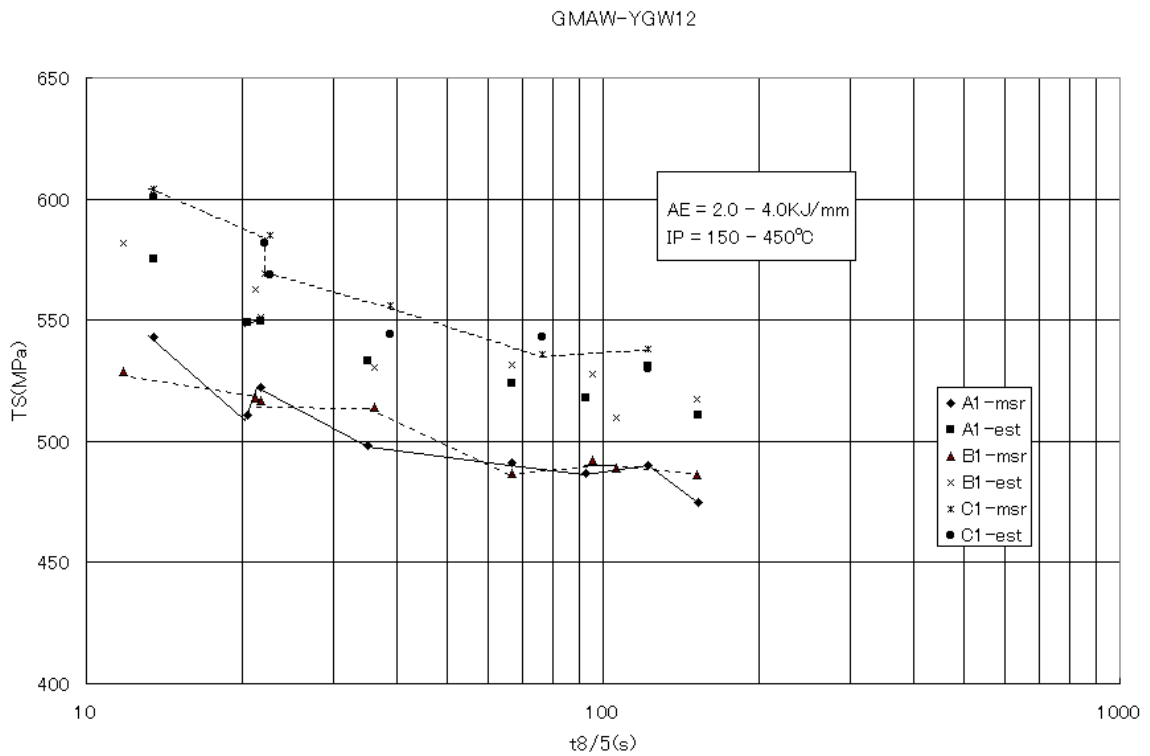


Fig.6 GMAW(YGW12) weld metal tensile strengths measured and predicted

GMAW-YGW17

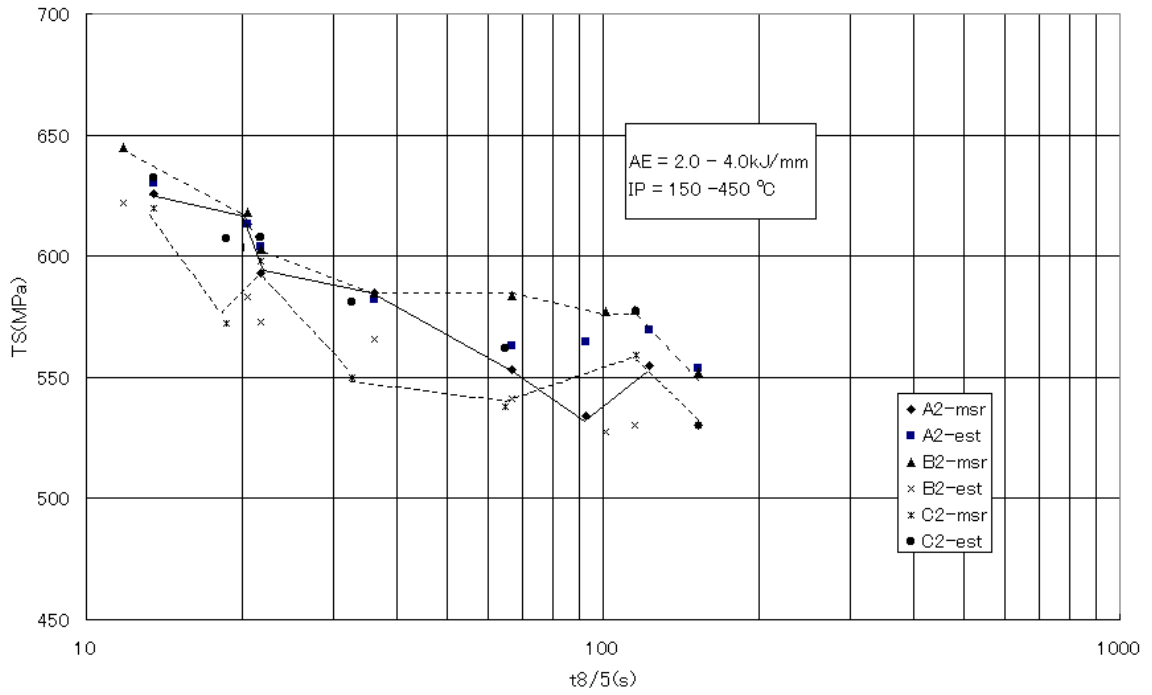


Fig.7 GMAW(YGW17) weld metal tensile strengths measured and predicted

GMAW-YGW21

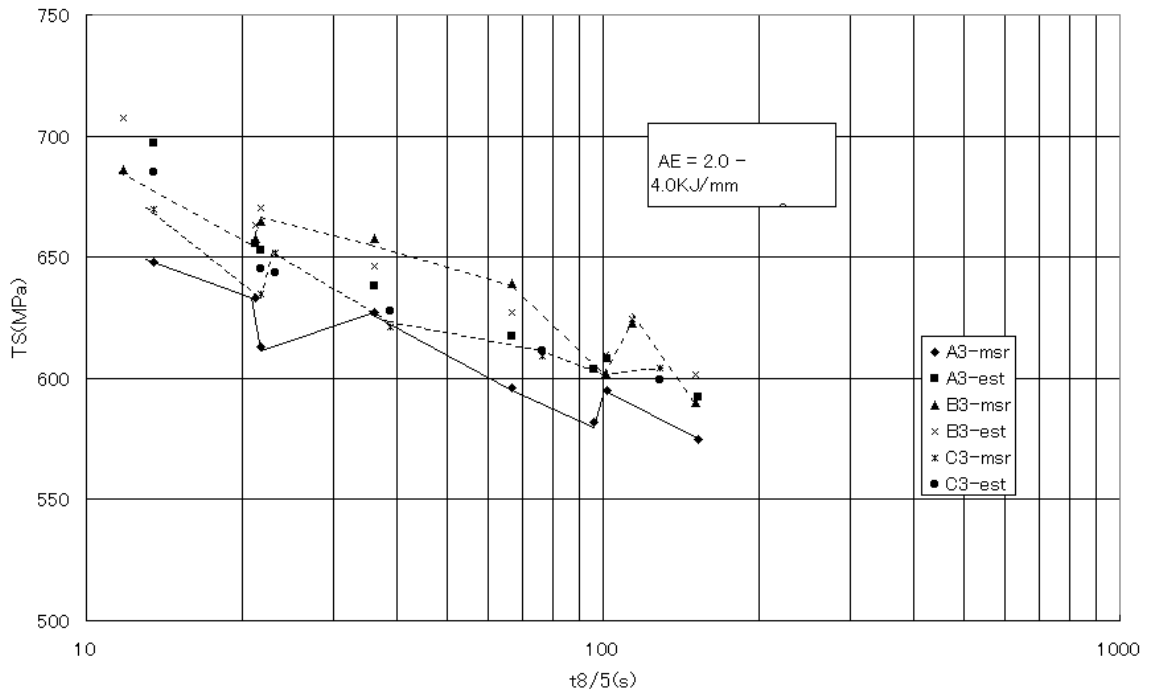


Fig.8 GMAW(YGW21) weld metal tensile strengths measured and predicted

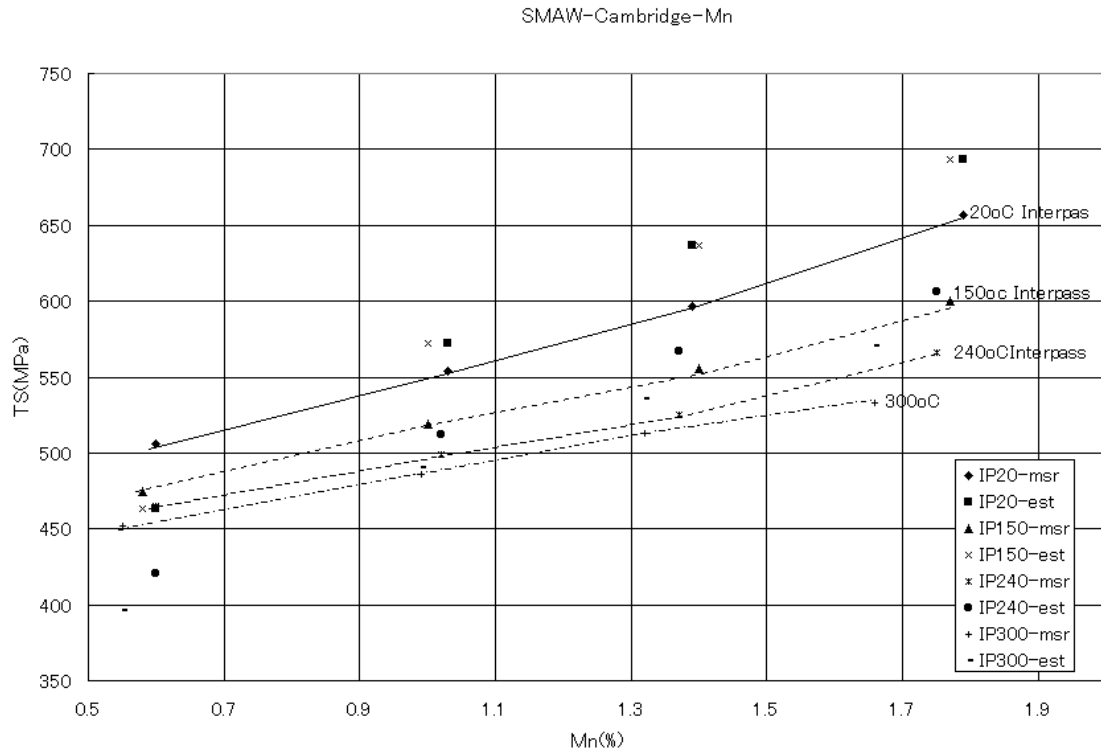


Fig.9 SMAW (U. Cambridge) tensile strengths measured and predicted against Mn content

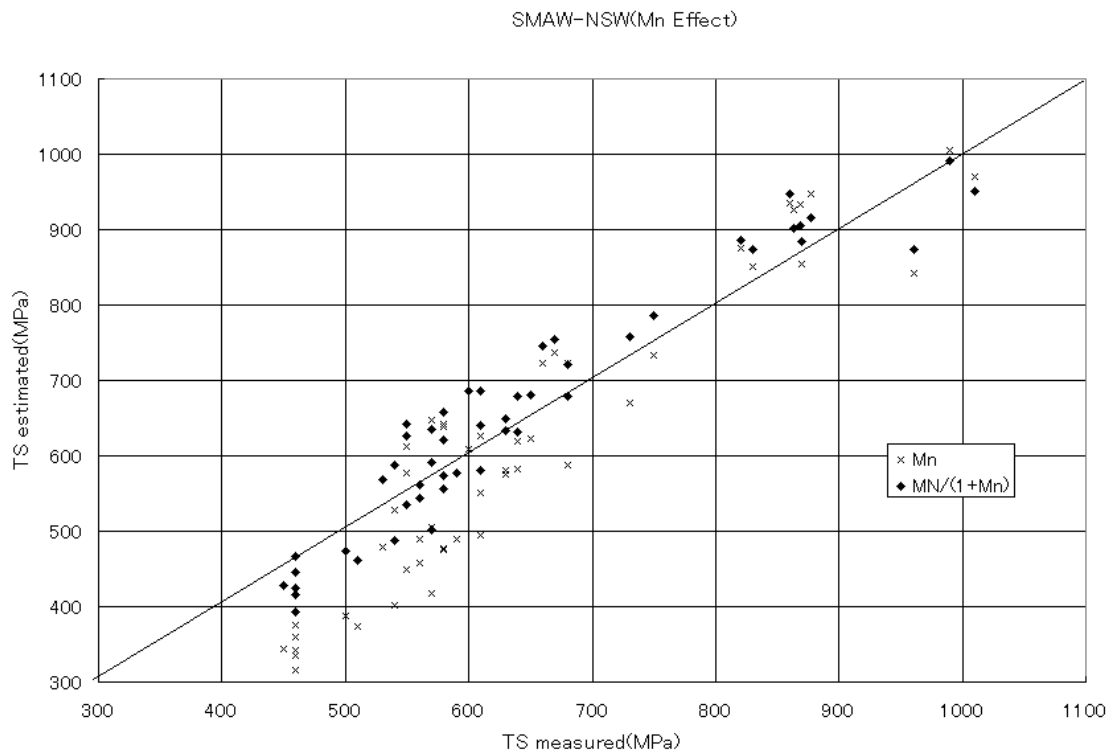


Fig.10 Predicted tensile strengths of SMAW (U. Cambridge) with linear and non-linear

Mn effect considered

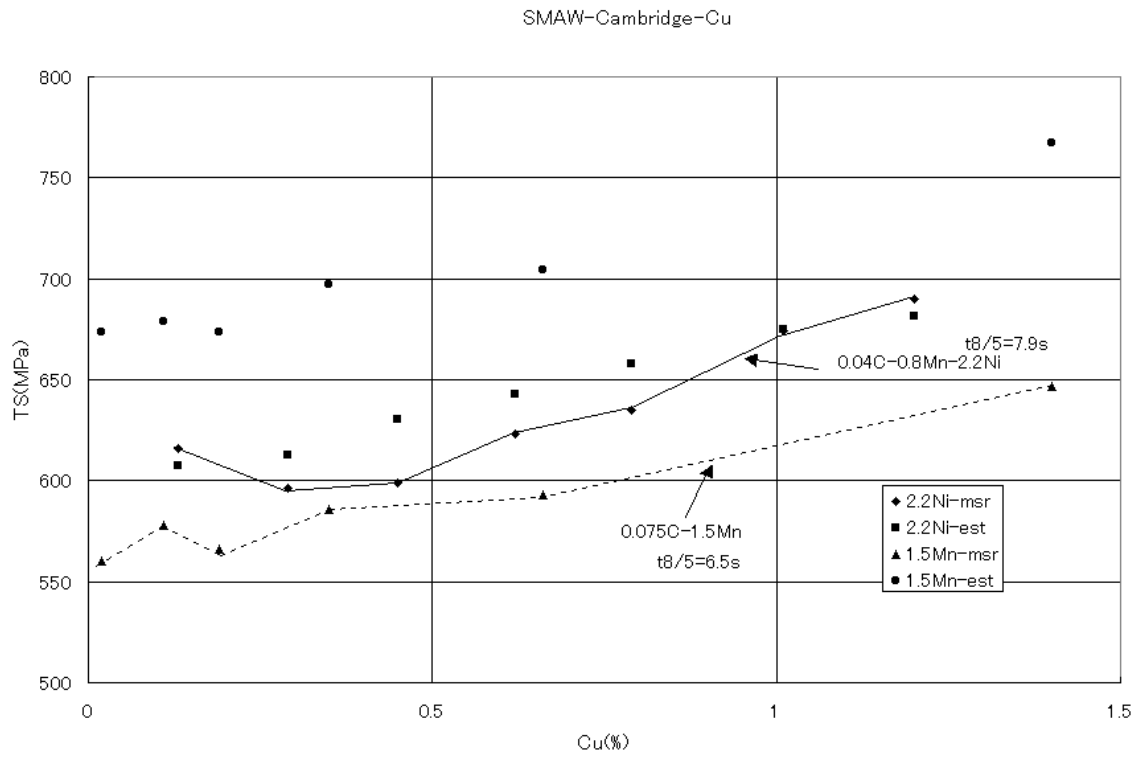


Fig.11 SMAW (U. Cambridge) tensile strengths measured and predicted against Cu content

SMAW-Cambridge-Ni

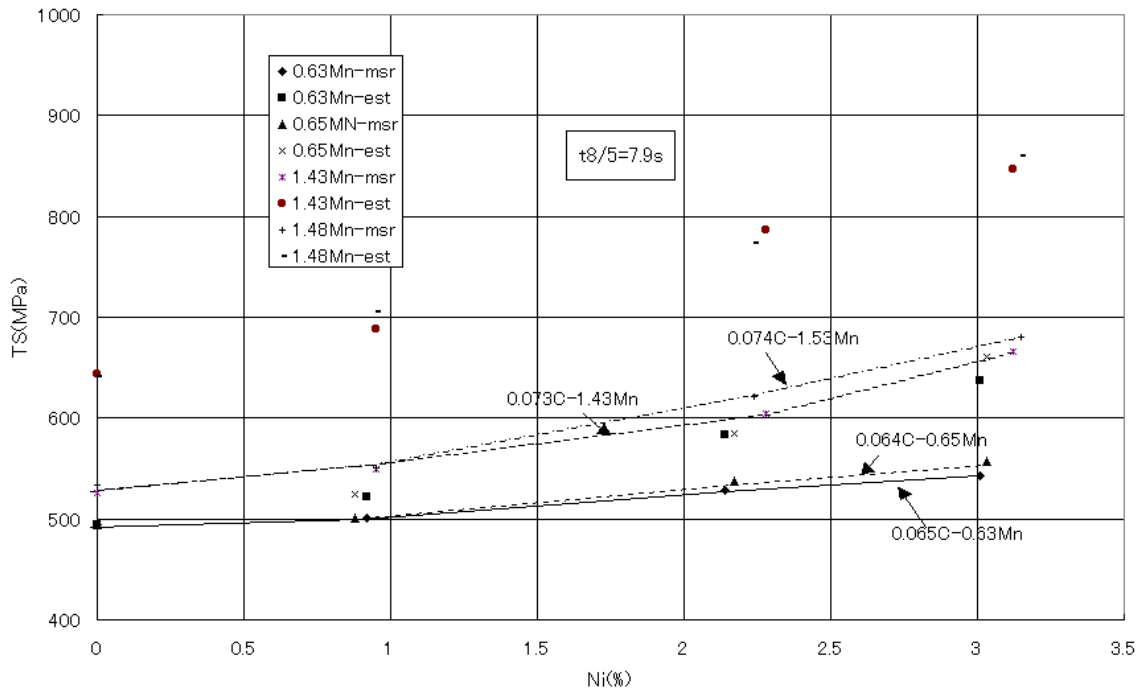


Fig.12 SMAW (U. Cambridge) tensile strengths measured and predicted against Ni content

SMAW-Cambridge-Cr

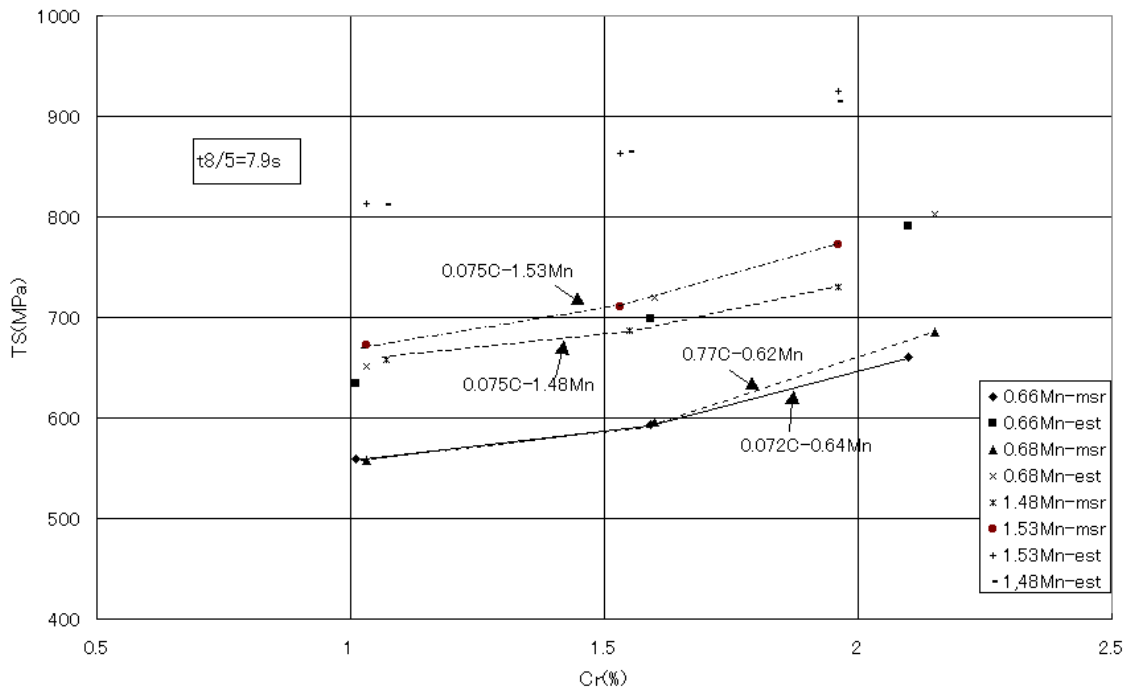


Fig.13 SMAW (U. Cambridge) tensile strengths measured and predicted against Cr content

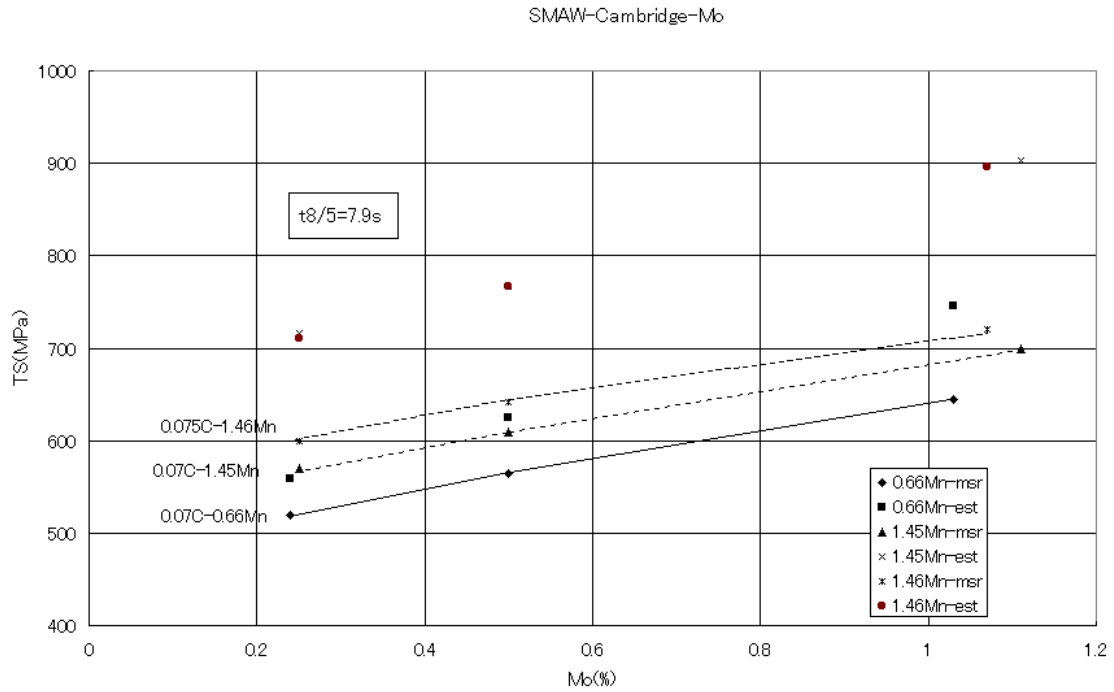


Fig.14 SMAW (U. Cambridge) tensile strengths measured and predicted against Mo content

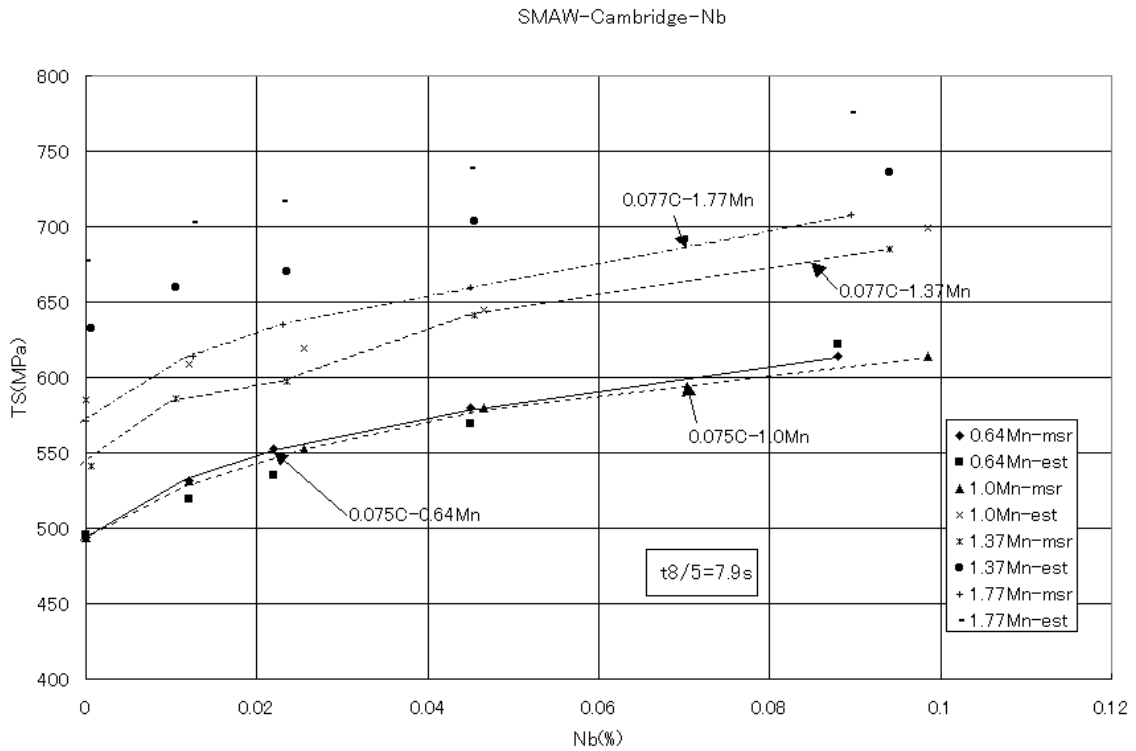




Fig.15 SMAW (U. Cambridge) tensile strengths measured and predicted against Nb content

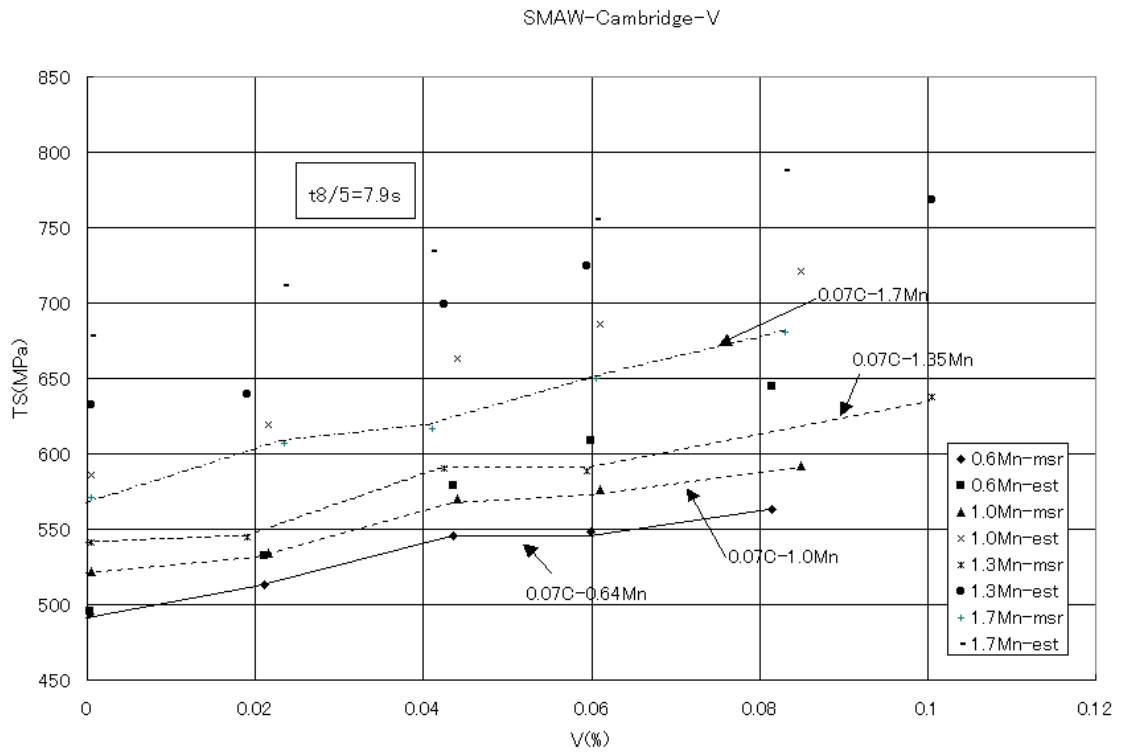


Fig.16 SMAW (U. Cambridge) tensile strengths measured and predicted against V content

## Appendix Calculation of welding cooling time, $t_{8/5}$

It is important to precisely calculate welding cooling time,  $t_{8/5}$  from welding conditions of arc energy, thickness and preheat and inter-pass temperature in order to predict the hardness and tensile strength of a weld metal with higher accuracy.

### A1. Welding heat conduction equation

A welding heat conduction formula in the present study is based on a Rothenthal basic equation<sup>A1)</sup>. But the formula additionally includes the effect of the finite plate thickness, the preheating temperature and heat transfer from the surfaces of a weld and a plate as follows:

$$T = T_{\infty} + T_w \cdot \exp\left\{\left(-\frac{\alpha_1}{\rho c}\right) \cdot \left(\frac{2t}{h}\right)\right\} + (T_{ph} - T_{\infty}) \exp\left\{\left(-\frac{\alpha_2}{\rho c}\right) \left(\frac{2t}{h}\right)\right\} \quad \bullet A1 \bullet$$

$$T_w = \frac{Q_p}{2\pi\lambda} \exp\left(\frac{-vw}{2\kappa}\right) \left[ \frac{\exp(-vR/2\kappa)}{R} + \sum_{n=1}^{\infty} r^n \left\{ \frac{\exp(-vR_n/2\kappa)}{R_n} + \frac{\exp(-vR'_n/2\kappa)}{R'_n} \right\} \right] \quad \bullet A2 \bullet$$

where,  $T$ : temperature ( $^{\circ}\text{C}$ ),  $T_{ph}$ : preheat and inter-pass temperature ( $^{\circ}\text{C}$ ),  $T_{\infty}$ : ambient temperature ( $^{\circ}\text{C}$ ),  $T_w$ : temperature increase due to moving point heat source ( $^{\circ}\text{C}$ ),  $x$ : co-ordinate in the welding direction (cm),  $z$ : co-ordinate in the plate thickness direction (cm),  $y$ : co-ordinate in the direction perpendicular to the welding direction (cm),  $t$ : time (s) after a point heat source passed at the point ( $x=y=z=0$ ),

$$R: R = \sqrt{w^2 + y^2 + z^2} \quad R_n: R_n = \sqrt{w^2 + y^2 + (2nh - z)^2} \quad R'_n: R'_n = \sqrt{w^2 + y^2 + (2nh + z)^2}$$

$Q_p$ : Efficient energy of heat source =  $0.24 \eta AV$  (cal/s),  $h$ : plate thickness (cm),

$\eta$ : arc efficiency = 1.0 (SAW), 0.80 (SMAW, GMAW),

$\alpha_1/\rho c$ : surface heat transfer coefficient at a weld = 0.0005 cm/s (SAW)  
= 0.0020 cm/s (SMAW, GMAW),

GMAW),

$\alpha_2/\rho c$ : surface heat transfer coefficient at a plate = 0.0020 cm/s

$r$ : heat reflection rate at the surface = 0.90 (SAW), 0.80 (SMAW, GMAW),

$\lambda$ : heat conduction =  $0.06 + 0.000012 HI$  (cal/cm s)

$\kappa$ : heat diffusivity=0.042+0.000016 HI (cm cm/s)

$E$ : arc energy= 60 A V /v (J/cm)

HI: Heat input =  $\eta E$  (J/cm)

A: welding current(A)

V: welding voltage (V)

The heat conduction equation, Eq. (A2) includes a heat reflection term,  $r^n$ . Consequently, this equation does not satisfy the boundary condition of Eq. (A3) in a strict sense. If  $r=1.0$  is considered, then the boundary condition is satisfied but the effect of the thickness becomes excessive resulting in unsatisfactory prediction of experimental data. So,  $r=0.90$  for SAW and  $r=0.80$  for SMAW and GMAW in this study.

$$\lambda \frac{\partial T}{\partial z} = -\alpha(T - T_{\infty}) \quad (A3)$$

## A2. Comparison of calculation and experiments

Table A1 shows the comparison of calculation and experiments<sup>A2)</sup> of  $t_{8/5}$  in SMAW.

Table A1  $t_{8/5}$  calculated and measured in SMAW

Welding condition				Welding cooling time, $t_{8/5}$ (s)	
• (kJ/mm)	Welding condition	Thick(mm)	Preheat(°C)	Experiment	Calculation
8.0	120A, 24V, 21.5cpm	9	20	5.8	4.9
			100	6.7, 7.2, 7.6	7.8
			185	11.0, 12.6, 12.1	12.3
		16	20	3.1, 3.1, 3.3	3.6
			100	4.0, 4.0, 4.3	4.8
			200	6.6, 6.8, 6.5	7.1
		20	20	2.8, 3.1, 3.3	3.6
			100	4.0, 4.2, 4.2	4.8
			200	6.5, 6.6, 6.2	7.1
17	170A, 25V, 15cpm	9	20	16.4, 22.1, 21.5	19.8
			100	26.2, 33.0, 28.2	27.0
			200	34.2, 41.0, 37.0	38.2

		16	20	8.2, 10.6	7.7
			100	10.2, 11.6, 12.1	11.3
			200	18.2, 21.6, 20.7	18.9
		20	20	6.9, 7.1	6.8
			100	9.1, 9.9	8.7
			200	13.8, 15.0, 15.8	15.2
45	285A, 29V, 11cpm	9	20	62.0, 74.7	68.0
			100	75.3	81.6
			200		88.2
		16	20	31.1	46.3
			100	46.5	59.3
			200	59.0, 70.6	82.2
		20	20	20.7, 28.4	28.6
			100	40.2, 35.6	44.8
			200	53.6, 46.7	69.3

Table A2 shows  $t_{8/5}$  calculated and measured for SAW.

Table A2  $t_{8/5}$  calculated and measured for SAW

Welding condition				Welding cooling time, $t_{8/5}$ (s)		
• (kJ/mm)	Welding condition	Thick(mm)	Preheat(°C)	Measurement	Calculation	Reference
10	400A, 25V, 60cpm	7.5	20	21, 19	18.1	A2
		10		13, 11	10.6	
		20		4.8	5.1	
		25		4.2	5.1	
		30		4.2	5.1	
		40		4.2	5.1	
20	400A, 25V, 30cpm	10	20	49, 47	38.7	A2
		12.5		21	28.2	
		15		16	17.7	
		20		10	10.6	
		25		9	10.6	
		30		9	10.6	
30	400A, 25V, 20cpm	15	20	50, 43	43.1	A2
		17.5		33	31.0	
		20		27	21.2	
		25		18, 16	16.6	
		30		14	14.7	
10	400A, 25V, 60cpm	7.5	150	33	30.2	A2
		10		19	21.0	

		15		12	9.6	
		20		8	8.3	
		25		8	8.3	
20	400A, 25V, 30cpm	10		71, 63	56.2	
		15		38	37.4	
		20		22	20.5	
		25		15	16.5	
		30		15	16.5	
		40		15	16.5	
30	400A, 25V, 20cpm	15		70, 65	69.6	
		20		42	45.1	
		25		30, 28	28.5	
		30		23	25.7	
		40		23	22.9	
16		25	20	7	8.3	A3
29		25		18	14.7	
60		25		65	61.1	

Fig.A1 shows the comparison of measurements and experiments shown in Tables A1 and A2. Preferable coincidence was obtained. Consequently, the heat conduction formula and adopted thermal property values in the present study are considered satisfactory. A website is provided which enables to calculate easily  $t_{8/5}$  based on the present equation<sup>A5)</sup>.

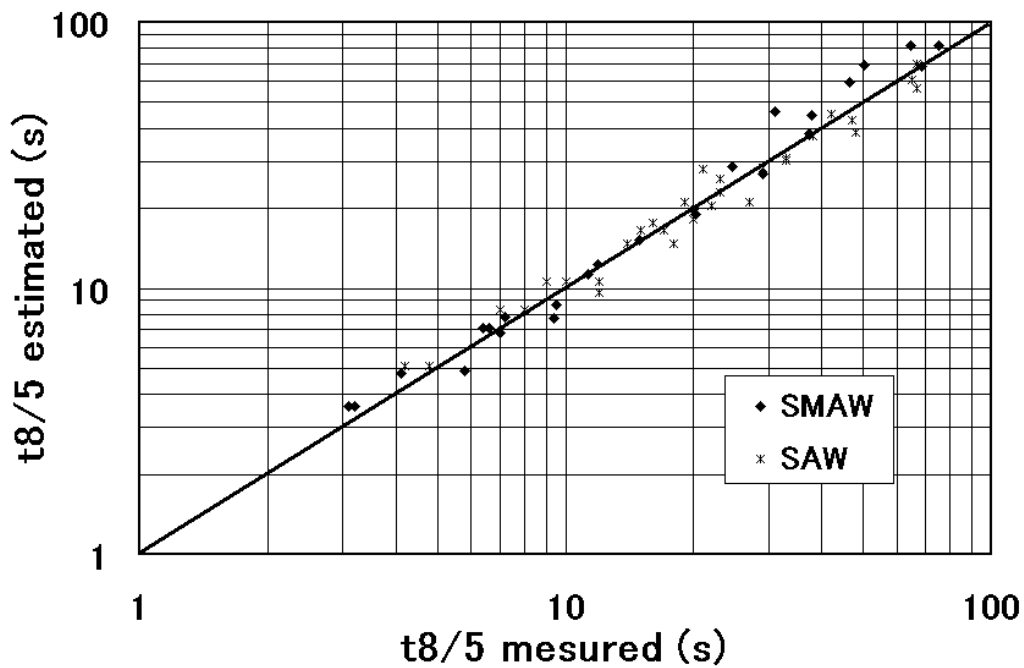


Fig. A1 Comparison of  $t_{8/5}$  calculated and measured

## References

- A1) D. Rosenthal: Mathematical Theory of Heat Distribution during Welding and Cutting, Weld. Journal, 20 (1941), 220s
- A2) N. Yurioka, M. Okumura, T. Kasuya, H. Cotton : Prediction of HAZ Hardness of Transformable Steels, Metal Const. 19 (1987), 139R
- A3) D. Uwer, J. Degenkolbe : Temperaturzyklen beim Lichtbogenschweissen - Berechnung von Abkühlzeiten, Schweissen und Schneiden, 24(1972), p485
- A4) R. Kohno, S. B. Jones, TWI Research Report S1/1978/PE (1978)
- A5) N. Yurioka : Nippon Steel Weldability Calculation  
<http://member.nifty.ne.jp/yurioka/index.html>



No	Exp.No	steel	welding	Arc energy (kJ/mm)	Interpass Temp(°C)	location	Estimated t8/5(s)	YS (MPa)	TS (MPa)	H v	C	Si	Mn	Cu	Ni	Cr	Mo	Nb	V	T.Ti	T.Al	B (ppm)	N (ppm)	O (ppm)	CE(IIW)
63	C44	EH36(40t)	Each Side	13.7	150	2nd side	197	520	588	189	0.090	0.19	1.39	0.20	0.21	0	0.07	0.008	0.036	0.012	0.008	25	37	233	0.370
64	C54						197	560	634	207	0.091	0.18	1.31	0.21	0.19	0	0.22	0.009	0.038	0.012	0.008	25	38	246	0.388
65	D34						197	502	566	173	0.092	0.19	1.50	0.21	0.21	0	0	0.009	0.035	0.014	0.007	28	37	244	0.377
66	D44						197	536	608	198	0.096	0.19	1.49	0.21	0.20	0	0.12	0.009	0.037	0.013	0.007	28	36	241	0.403
67	D54						197	536	652	208	0.093	0.18	1.50	0.21	0.19	0	0.25	0.008	0.035	0.013	0.008	28	36	214	0.427
68	D64						197	550	676	217	0.092	0.18	1.42	0.21	0.22	0	0.36	0.008	0.036	0.012	0.008	28	37	238	0.437
69	E44						197	571	647	203	0.089	0.21	1.65	0.19	0.20	0	0.11	0	0.036	0.015	0.008	27	40	231	0.419
70	E54						197	570	676	212	0.092	0.21	1.67	0.21	0.21	0	0.21	0.008	0.036	0.014	0.009	28	39	233	0.448
71	M81	EH36(25t)		8.36	150		162	576	664	216	0.079	0.20	1.45	0.18	0.44	0	0.16	0.008	0.043	0.014	0.008	33	34	194	0.403
72	M82						162	571	671	217	0.077	0.20	1.47	0.18	0.42	0	0.16	0.008	0.045	0.014	0.007	45	36	195	0.403
73	M83						162	578	671	218	0.074	0.20	1.48	0.18	0.43	0	0.16	0.008	0.044	0.014	0.008	41	35	200	0.402
74	D72						162	485	582	187	0.083	0.21	1.39	0.19	0.19	0	0.08	0.005	0.035	0.014	0.009	29	33	223	0.363
75	D82						162	563	622	198	0.084	0.22	1.33	0.20	0.19	0	0.15	0.006	0.036	0.014	0.009	28	34	219	0.369
76	D74	EH36(40t)		13.6	150		197	492	601	188	0.092	0.20	1.49	0.21	0.19	0	0.06	0.005	0.035	0.013	0.008	28	38	212	0.386
77	D84						197	557	627	194	0.092	0.21	1.51	0.22	0.26	0	0.12	0.005	0.036	0.012	0.009	25	38	214	0.407
78	B42	EH36(25t)		8.36	150		162	489	563	180	0.081	0.19	1.07	0.20	0.20	0	0.12	0.004	0.040	0.012	0.008	25	32	258	0.318
79	B72						162	481	554	176	0.083	0.20	1.09	0.20	0.20	0	0.01	0.004	0.038	0.014	0.009	18	28	238	0.301
80	E32						162	486	579	182	0.082	0.24	1.60	0.18	0.20	0	0	0.004	0.037	0.015	0.01	28	29	212	0.381
81	E72						162	531	621	196	0.080	0.22	1.58	0.18	0.20	0	0.07	0.005	0.037	0.014	0.009	25	31	222	0.390
82	C62						162	563	644	210	0.080	0.19	1.18	0.20	0.20	0	0.45	0.004	0.036	0.012	0.008	21	27	263	0.401
83	B44	EH36(40t)		13.7	150		197	478	559	188	0.092	0.19	1.14	0.21	0.20	0	0.09	0.004	0.035	0.012	0.009	20	37	224	0.334
84	B74						197	471	544	172	0.086	0.19	1.18	0.22	0.20	0	0.06	0.004	0.037	0.012	0.009	22	36	248	0.330
85	E34						197	480	583	185	0.094	0.22	1.67	0.20	0.20	0	0	0.005	0.039	0.014	0.009	29	40	225	0.407
86	E74						197	521	617	195	0.090	0.23	1.64	0.20	0.20	0	0.06	0.004	0.037	0.012	0.009	21	40	227	0.409
87	B52	EH36(25t)		8.36	150		162	541	600	196	0.095	0.18	1.08	0.20	0.20	0	0.28	0.006	0.036	0.013	0.010	26	44	280	0.365
88	E42						162	532	649	207	0.083	0.23	1.62	0.18	0.20	0	0.11	0.009	0.037	0.015	0.010	26	31	222	0.408
89	E52						162	579	680	218	0.087	0.22	1.56	0.15	0.20	0	0.29	0.009	0.038	0.016	0.009	28	33	214	0.436
90	AY1	WT950(75t)	V-groove	3.5	150	10mm	27	911	978	320	0.08	0.16	1.44	0.10	2.85	1.00	1.03	0.003	0.007	0.009	0.025	5	15	255	0.924
91	AU1					beneath	27	892	997	330	0.07	0.15	1.43	0.07	2.85	0.90	0.90	0.002	0.006	0.009	0.025	5	13	269	0.864
92	AY2						27	780	969	305	0.07	0.18	1.44	0.08	2.88	0.99	0.99	0.003	0.007	0.008	0.025	5	11	262	0.905
93	Au2						27	862	974	310	0.08	0.17	1.41	0.09	2.58	0.98	0.98	0.003	0.007	0.008	0.025	5	10	312	0.886
94	AY3			4.5	150		36	777	981	315	0.07	0.13	1.43	0.08	2.94	0.90	0.90	0.002	0.007	0.009	0.025	5	12	245	0.871
95	AU3						36	797	992	320	0.08	0.12	1.43	0.09	2.85	0.92	0.92	0.002	0.007	0.009	0.025	5	17	275	0.884
96	AY4			3.5	150		27	841	990	315	0.07	0.14	1.42	0.08	2.59	1.02	1.00	0.002	0.005	0.009	0.025	5	17	240	0.890
97	AY5			4.5	150		36	784	998	320	0.08	0.15	1.50	0.09	2.61	1.04	0.99	0.003	0.007	0.008	0.025	5	11	294	0.917
98	AY6			5.5	150		41	766	995	330	0.08	0.14	1.43	0.09	2.64	1.04	1.00	0.003	0.006	0.007	0.025	5	11	262	0.910
99	AY7						41	810	982	322	0.08	0.13	1.40	0.10	2.60	0.98	1.01	0.002	0.008	0.008	0.025	5	17	237	0.893
100	AY8			6.0	150		45	774	1001	330	0.08	0.14	1.43	0.08	2.64	1.06	1.00	0.003	0.006	0.008	0.025	5	14	236	0.913
101	AY9						45	898	985	325	0.08	0.15	1.39	0.08	2.59	1.01	1.03	0.002	0.005	0.008	0.025	5	15	230	0.899

Hatched: Estimated











No	Product	Steel	Welding Process	Arc Energy (kJ/mm)	Interpass Temp(°C)	Estimated t8/5 (s)	YS (MPa)	TS (MPa)	YR (%)	Hv	C	Si	Mn	Cu	Ni	Cr	Mo	Nb	V	T.Ti	T.Al	B (ppm)	N (ppm)	O (ppm)	CE (IIW)
139	B333	SN490B 25mm	CO2, 6layer7pas	2.94	350	66.8	522	639	0.82	203	0.08	0.47	1.45	0.2			0.3			0.05	0.008	3	160		0.395
140	B334	SN490B 25mm	CO2, 6layer7pas	2.97	438	114	467	623	0.75	211	0.09	0.49	1.48	0.2			0.29			0.053	0.009	3	150		0.408
141	B343	SN490B 25mm	CO2, 5layer6pas	4.1	350	101	478	602	0.79	197	0.07	0.46	1.41	0.2			0.32			0.048	0.007	3	100		0.382
142	B344	SN490B 25mm	CO2, 5layer6pas	4.01	447	151	429	590	0.73	185	0.08	0.44	1.4	0.2			0.28			0.044	0.008	3	100		0.383
143	C321	SN490B 25mm	CO2, 7layer10pas	2.03	150	13.5	594	670	0.89	224	0.08	0.55	1.41	0.2			0.24			0.041	0.007	3	90		0.376
144	C322	SN490B 25mm	CO2, 8layer11pas	2.01	250	21.8	548	635	0.86	214	0.07	0.57	1.39	0.2			0.26			0.039	0.006	3	80		0.367
145	C331	SN490B 25mm	CO2, 6layer7pas	3.18	150	23.2	565	652	0.87	207	0.08	0.51	1.32	0.2			0.25			0.039	0.007	2	140		0.363
146	C332	SN490B 25mm	CO2, 6layer7pas	3.23	250	38.7	523	621	0.84	209	0.08	0.55	1.4	0.2			0.23			0.042	0.008	3	80		0.373
147	C333	SN490B 25mm	CO2, 6layer7pas	3.23	350	76.1	478	609	0.78	199	0.07	0.6	1.46	0.2			0.25			0.048	0.007	2	110		0.377
148	C334	SN490B 25mm	CO2, 6layer7pas	3.14	450	129	450	604	0.75	195	0.08	0.54	1.37	0.2			0.25			0.041	0.007	2	150		0.372
149	C343	SN490B 25mm	CO2, 6layer6pas	4.05	350	101	388	527	0.74	178	0.08	0.4	1.1	0.2			0.25			0.028	0.006	3	120		0.327
150	C344	SN490B 25mm	CO2, 6layer6pas	3.85	450	145	390	540	0.72	164	0.08	0.43	1.15	0.2			0.24			0.031	0.006	2	90		0.333
151	D321	SN490B 25mm	CO2, 6layer10pas	2	149	13.5	563	648	0.87	220	0.07	0.53	1.5	0.2			0.22			0.038	0.012	2	130		0.377
152	D322	SN490B 25mm	CO2, 6layer9pas	2.06	249	21.7	542	632	0.86	210	0.07	0.53	1.49	0.2			0.23			0.04	0.011	2	130		0.378
153	D331	SN490B 25mm	CO2, 5layer7pas	3.06	149	20.4	532	624	0.85	224	0.07	0.46	1.39	0.2			0.21			0.035	0.011	1	140		0.357
154	D332	SN490B 25mm	CO2, 5layer7pas	2.98	249	35.9	496	609	0.81	206	0.08	0.48	1.43	0.2			0.21			0.035	0.01	2	100		0.374
155	D333	SN490B 25mm	CO2, 5layer7pas	2.91	348	66.6	479	597	0.8	193	0.07	0.49	1.45	0.2			0.2			0.038	0.012	1	190		0.365
156	D334	SN490B 25mm	CO2, 5layer7pas	2.95	443	115	420	571	0.74	182	0.08	0.48	1.42	0.2			0.2			0.032	0.01	2	80		0.37
157	D343	SN490B 25mm	CO2, 5layer5pas	3.98	339	94.6	443	574	0.77	187	0.08	0.46	1.4	0.2			0.2			0.036	0.012	1	120		0.367
158	D344	SN490B 25mm	CO2, 5layer5pas	3.94	427	134	409	569	0.72	178	0.08	0.48	1.42	0.2			0.2			0.038	0.011	2	140		0.37
159	E321	SN490B 25mm	CO2, 6layer8pas	2.17	150	14.6	624	702	0.89	234	0.09	0.63	1.54	0.2			0.21			0.049	0.008	6	100		0.402
160	E322	SN490B 25mm	CO2, 6layer8pas	2.16	250	23.9	596	682	0.87	224	0.09	0.6	1.55	0.2			0.19			0.049	0.01	6	130		0.4
161	E331	SN490B 25mm	CO2, 5layer6pas	3.02	150	20.5	582	672	0.87	228	0.09	0.6	1.5	0.2			0.2			0.049	0.01	6	130		0.393
162	E332	SN490B 25mm	CO2, 5layer6pas	3.18	249	38.6	545	649	0.84	216	0.09	0.56	1.43	0.2			0.2			0.039	0.008	5	130		0.382
163	E333	SN490B 25mm	CO2, 5layer6pas	3	350	66.8	535	676	0.79	221	0.09	0.64	1.58	0.2			0.19			0.058	0.008	6	130		0.405
164	E334	SN490B 25mm	CO2, 5layer6pas	3	390	92.2	502	672	0.75	208	0.1	0.62	1.6	0.2			0.18			0.057	0.012	6	100		0.416
165	E343	SN490B 25mm	CO2, 4layer5pas	4.1	350	101	479	633	0.76	203	0.09	0.57	1.55	0.2			0.18			0.044	0.01	6	80		0.398
166	E344	SN490B 25mm	CO2, 4layer5pas	4.2	438	150	435	609	0.71	194	0.1	0.56	1.5	0.2			0.17			0.042	0.01	6	110		0.397
167	G321	SN490B 25mm	CO2, 6layer9pas	2.01	150	13.5	604	676	0.89	232	0.08	0.61	1.43	0.2			0.24			0.049	0.005	5	40		0.38
168	G322	SN490B 25mm	CO2, 5layer7pas	2.03	250	21.8	563	647	0.87	219	0.08	0.58	1.44	0.2			0.23			0.043	0.004	4	60		0.379
169	G331	SN490B 25mm	CO2, 5layer6pas	3.05	150	20.5	552	637	0.87	224	0.08	0.57	1.38	0.2			0.24			0.036	0.005	4	60		0.371
170	G332	SN490B 25mm	CO2, 5layer6pas	3.06	250	35.1	488	604	0.81	213	0.08	0.53	1.39	0.2			0.22			0.037	0.005	3	40		0.369
171	G333	SN490B 25mm	CO2, 5layer6pas	3.04	350	71	456	584	0.78	197	0.09	0.52	1.35	0.2			0.22			0.033	0.004	4	50		0.372
172	G334	SN490B 25mm	CO2, 5layer6pas	3.06	430	113	415	583	0.71	185	0.08	0.55	1.38	0.2			0.22			0.039	0.004	4	60		0.367
173	G343	SN490B 25mm	CO2, 5layer5pas	4.08	350	101	429	580	0.74	182	0.09	0.51	1.38	0.2			0.2			0.034	0.005	4	40		0.373
174	G344	SN490B 25mm	CO2, 5layer5pas	4.1	450	152	411	574	0.72	184	0.08	0.52	1.35	0.2			0.22			0.034	0.005	3	60		0.362

Table 4 Chemical Composition and Mechanical Properties of SMAW

No	Product	Steel	Welding Process	Arc Energy (kJ/mm)	Interpas Temp(degC)	Estimate t8/5 (s)	YS (MPa)	TS (MPa)	YR (%)	EL (%)	C	Si	Mn	Cu	Ni	Cr	Mo	Nb	V	T.Ti	T.Al	B (ppm)	N (ppm)	O (ppm)	CE(IIW)
1	G200(NSW)	All weld me	(Multi-run	1.30	100	7.6	390	450	0.87	31	0.070	0.08	0.46												0.147
2	B1(NSW)			1.30	100	7.6	410	460	0.89	31	0.090	0.10	0.42												0.160
3	A200(NSW)			1.30	100	7.6	410	460	0.89	30	0.080	0.12	0.40												0.147
4	G300(NSW)			1.30	100	7.6	400	460	0.87	32	0.080	0.13	0.53												0.168
5	A1(NSW)			1.30	100	7.6	400	460	0.87	30	0.060	0.18	0.38												0.123
6	EX-3A(NSW)			1.30	100	7.6	440	460	0.96	33	0.070	0.16	0.41												0.138
7	L16(NSW)			1.70	100	8.7	460	540	0.85	34	0.070	0.58	1.10												0.253
8	L16W(NSW)			1.60	100	8.3	480	580	0.83	32	0.070	0.61	0.90												0.220
9	L55(NSW)			1.70	100	8.7	480	550	0.87	32	0.070	0.62	1.18												0.267
10	L16LH(NSW)			1.70	100	8.7	440	510	0.86	34	0.050	0.48	0.64												0.157
11	L60(NSW)			1.70	100	8.7	540	640	0.84	29	0.070	0.42	1.12		0.73		0.22								0.349
12	L60S(NSW)			1.70	100	8.7	580	650	0.89	29	0.050	0.46	1.12		1.51		0.20								0.377
13	L62(NSW)			1.70	100	8.7	600	670	0.90	31	0.070	0.48	1.39		0.76		0.35								0.422
14	L60LT(NSW)			1.70	100	8.7	600	680	0.88	28	0.070	0.41	1.51		0.67		0.18			0.03		20			0.402
15	L80(NSW)			1.70	100	8.7	740	830	0.89	24	0.050	0.44	1.35		2.52	0.18	0.54								0.587
16	L80EL(NSW)			1.70	100	8.7	740	820	0.90	24	0.060	0.45	1.44		2.44	0.20	0.42								0.587
17	L80SN(NSW)			1.70	100	8.7	760	860	0.88	22	0.050	0.36	1.39		4.64		0.48								0.687
18	L60W(NSW)			1.70	100	8.7	550	630	0.87	31	0.070	0.6	1.02		0.51		0.19								0.312
19	L60G(NSW)			2.30	100	14.8	530	630	0.84	30	0.060	0.78	1.04		0.72		0.28								0.337
20	L62CF(NSW)			1.70	100	8.7	590	660	0.89	30	0.070	0.45	1.36		0.70		0.35								0.413
21	L70(NSW)			1.70	100	8.7	660	750	0.88	26	0.050	0.41	1.16		2.10		0.48								0.479
22	L85(NSW)			1.70	100	8.7	820	870	0.94	23	0.040	0.48	1.25		2.46	0.76	0.49								0.662
23	L100EL(NSW)			1.70	100	8.7	910	990	0.92	21	0.060	0.25	1.67		2.01	0.89	0.75								0.800
24	CT03Cr(NSW)			1.40	100	6.3	500	570	0.88	31	0.050	0.16	0.41	0.32	0.15	0.48									0.246
25	CT16Cr(NSW)			1.70	100	8.7	500	560	0.89	31	0.040	0.37	0.62	0.35	0.14	0.50									0.276
26	CT16VCr(NSW)			1.70	100	8.7	520	570	0.91	31	0.060	0.41	0.72	0.32	0.13	0.47									0.304
27	CT26GCr(NSW)			2.60	100	14.8	470	550	0.85	30	0.060	0.22	1.28	0.33	0.16	0.47									0.400
28	CT60Cr(NSW)			1.70	100	8.7	520	610	0.85	27	0.070	0.38	0.67	0.44	0.62	0.56									0.364
29	CT60GCr(NSW)			2.60	100	14.8	590	640	0.92	28	0.040	0.48	1.08	0.48	0.50	0.52									0.389
30	ST03(NSW)			1.40	100	8	440	500	0.88	30	0.070	0.10	0.50	0.35											0.177
31	ST16(NSW)			1.70	100	8.7	450	540	0.83	34	0.070	0.48	0.50	0.37											0.178
32	ST03Cr(NSW)			1.70	100	8.7	460	530	0.87	28	0.060	0.15	0.56	0.23		0.79									0.327
33	ST16Cr(NSW)			1.70	100	8.7	480	550	0.87	29	0.050	0.50	0.48	0.20		0.73									0.289
34	RS55(NSW)			1.70	100	8.7	500	590	0.85	28	0.050	0.53	0.57			1.00									0.345
35	RS55G(NSW)			1.70	100	8.7	540	610	0.89	26	0.050	0.62	0.52	0.18		0.73	0.13								0.321
36	L55SN(NSW)			1.70	100	8.7	530	580	0.91	30	0.070	0.42	1.41		0.57					0.02		20			0.343
37	N11(NSW)			1.70	100	8.7	540	610	0.89	31	0.070	0.49	1.15		1.62										0.370
38	N12(NSW)			1.70	100	8.7	520	600	0.87	30	0.060	0.44	1.02		2.38										0.389
39	N13(NSW)			1.70	100	8.7	500	580	0.86	31	0.050	0.42	0.46		3.35										0.350
40	N17(NSW)			1.70	100	8.7	670	730	0.92	21	0.040	0.14	0.26		7.91										0.611
41	N110(NSW)			1.70	100	8.7	520	570	0.91	31	0.070	0.21	1.57							0.03		30			0.332
42	L55S(NSW)			1.70	100	8.7	460	560	0.82	29	0.070	0.45	0.98												0.233
43	N16(NSW)			1.70	100	8.7	600	680	0.88	23	0.040	0.17	0.28			6.65									0.530
44	N118(NSW)			1.70	100	8.7	520	580	0.90	30	0.060	0.23	1.60							0.03		40			0.327
45	Tifree1(Kobe)			2.40	120	14.5	898	1010	0.889		0.049	0.38	1.72		2.5	0.87	0.85			0.003	0.008		130	170	0.846
46	Tifree2(Kobe)			1.73	120	10.1	729	869	0.839	22	0.041	0.58	1.77		2.71		0.78			0.002			120	260	0.673
47	Tibear1(Kobe)			1.73	120	10.1	727	863	0.842	23	0.040	0.52	1.73		2.78		0.79						150	220	0.672
48	Tibear2(Kobe)			2.40	120	14.5	873	961	0.908		0.048	0.4	1.25		2.51	0.74	0.64			0.015	0.005		180	210	0.700
49	Ti-B(Kobe)			1.73	120	10.1	793	877	0.904	24	0.039	0.64	1.84		2.83		0.82			0.016		34	100	220	0.698











No	Weld ID	Process	Arc Eneg (kJ/mm)	IP (oC)	t/8/5-est (s)	PWHT (oC)	PWHT (hr)	YS (MPa)	TS (MPa)	Hv	C	Si	Mn	Cu	Ni	Cr	Mo	Nb	V	Ti	Al	B (ppm)	N (ppm)	O (ppm)	CE(IIW)
1536	EvansLette	MMA	1	200	7.9	250	14	477	557		0.067	0.3	0.65	0	3.03	0	0	0	0	0.0036		0	72	460	
1539	EvansLette	MMA	1	200	7.9	250	14	436	519		0.069	0.33	0.68	0	0	0	0.24	0	0	0.0036		0	67	395	
1542	EvansLette	MMA	1	200	7.9	250	14	483	565		0.073	0.34	0.66	0	0	0	0.5	0	0	0.0042		0	70	433	
1545	EvansLette	MMA	1	200	7.9	250	14	565	644		0.072	0.32	0.66	0	0	0	1.03	0	0	0.004		0	76	411	
1548	EvansLette	MMA	1	200	7.9	250	14	490	558		0.077	0.32	0.66	0	0	1.03	0	0	0	0.0034		0	75	457	
1551	EvansLette	MMA	1	200	7.9	250	14	509	596		0.078	0.26	0.62	0	0	1.6	0	0	0	0.0029		0	100	472	
1554	EvansLette	MMA	1	200	7.9	250	14	598	685		0.078	0.28	0.64	0	0	2.15	0	0	0	0.0042		0	95	482	
1557	EvansLette	MMA	1	200	7.9	250	14	417	498		0.063	0.3	0.64	0.53	0	0	0	0	0	0.0043		0	74	453	
1560	EvansLette	MMA	1	200	7.9	250	14	429	497		0.064	0.3	0.63	1.05	0	0	0	0	0	0.0042		0	65	456	
1563	EvansLette	MMA	1	200	7.9	250	14	516	568		0.066	0.37	0.67	1.44	0	0	0	0	0	0.0051		0	55	453	
1566	EvansLette	MMA	1	200	7.9	250	14	434	526		0.078	0.26	1.43	0	0	0	0	0	0	0.0005		0	86	481	
1569	EvansLette	MMA	1	200	7.9	250	14	470	550		0.073	0.28	1.39	0	0.95	0	0	0	0	0.0005		0	76	454	
1572	EvansLette	MMA	1	200	7.9	250	14	512	605		0.071	0.26	1.48	0	2.28	0	0	0	0	0.0005		0	87	460	
1575	EvansLette	MMA	1	200	7.9	250	14	573	666		0.073	0.24	1.43	0	3.12	0	0	0	0	0.0005		0	77	460	
1578	EvansLette	MMA	1	200	7.9	250	14	474	570		0.076	0.28	1.53	0	0	0	0.25	0	0	0.0005		0	84	444	
1581	EvansLette	MMA	1	200	7.9	250	14	523	610		0.076	0.25	1.45	0	0	0	0.5	0	0	0.0005		0	78	457	
1584	EvansLette	MMA	1	200	7.9	250	14	594	699		0.076	0.24	1.41	0	0	0	1.11	0	0	0.0005		0	85	447	
1587	EvansLette	MMA	1	200	7.9	250	14	570	658		0.08	0.28	1.48	0	0	1.07	0	0	0	0.0005		0	94	436	
1590	EvansLette	MMA	1	200	7.9	250	14	591	687		0.075	0.28	1.48	0	0	1.55	0	0	0	0.0005		0	86	466	
1593	EvansLette	MMA	1	200	7.9	250	14	637	730		0.076	0.28	1.44	0	0	1.96	0	0	0	0.0005		0	84	476	
1596	EvansLette	MMA	1	200	7.9	250	14	453	535		0.08	0.24	1.47	0.55	0	0	0	0	0	0.0005		0	96	455	
1599	EvansLette	MMA	1	200	7.9	250	14	492	566		0.075	0.24	1.41	1.06	0	0	0	0	0	0.0005		0	89	484	
1602	EvansLette	MMA	1	200	7.9	250	14	559	638		0.074	0.22	1.36	1.63	0	0	0	0	0	0.0005		0	110	484	
1605	EvansLette	MMA	1	200	7.9	250	14	460	533		0.074	0.28	1.46	0	0	0	0	0	0	0.0035		0	79	443	
1608	EvansLette	MMA	1	200	7.9	250	14	498	551		0.076	0.25	1.48	0	0.95	0	0	0	0	0.0033		0	81	417	
1611	EvansLette	MMA	1	200	7.9	250	14	555	622		0.068	0.27	1.46	0	2.24	0	0	0	0	0.0034		0	78	436	
1614	EvansLette	MMA	1	200	7.9	250	14	604	680		0.075	0.26	1.46	0	3.15	0	0	0	0	0.0032		0	72	418	
1617	EvansLette	MMA	1	200	7.9	250	14	560	600		0.076	0.26	1.49	0	0	0	0.25	0	0	0.0034		0	89	412	
1620	EvansLette	MMA	1	200	7.9	250	14	596	642		0.075	0.26	1.46	0	0	0	0.5	0	0	0.0031		0	86	429	
1623	EvansLette	MMA	1	200	7.9	250	14	650	720		0.075	0.25	1.44	0	0	0	1.07	0	0	0.0031		0	83	432	
1626	EvansLette	MMA	1	200	7.9	250	14	624	672		0.079	0.3	1.56	0	0	1.03	0	0	0	0.0027		0	98	431	
1629	EvansLette	MMA	1	200	7.9	250	14	650	710		0.073	0.29	1.53	0	0	1.53	0	0	0	0.0027		0	79	438	
1632	EvansLette	MMA	1	200	7.9	250	14	706	772		0.078	0.29	1.48	0	0	1.96	0	0	0	0.0028		0	82	438	
1635	EvansLette	MMA	1	200	7.9	250	14	495	557		0.076	0.27	1.48	0.53	0	0	0	0	0	0.0022		0	81	454	
1638	EvansLette	MMA	1	200	7.9	250	14	487	563		0.077	0.25	1.43	1.08	0	0	0	0	0	0.0019		0	92	456	
1641	EvansLette	MMA	1	200	7.9	250	14	570	625		0.069	0.25	1.37	1.6	0	0	0	0	0	0.0023		0	75	475	